Computers and Electronics in Agriculture 109 (2014) 109–123

Contents lists available at ScienceDirect

Computers and Electronics in Agriculture

journal homepage: www.elsevier.com/locate/compag

Automatic morphological trait characterization for corn plants via 3D holographic reconstruction

Supawadee Chaivivatrakul [a,b,*], Lie Tang [c], Matthew N. Dailey [b], Akash D. Nakarmi [c]

[a] Information Technology for Agriculture and Rural Development, Ubon Ratchathani University, Ubon Ratchathani 34190, Thailand
[b] Computer Science and Information Management, Asian Institute of Technology, Pathumthani 12120, Thailand
[c] Agricultural and Biological Systems Engineering, Iowa State University, Ames, IA 50011, United States

ARTICLE INFO

Article history:
Received 27 February 2014
Received in revised form 26 August 2014
Accepted 14 September 2014

Keywords:
Phenotyping
Trait characterization
3D holographic reconstruction
Corn plant
Point cloud data

ABSTRACT

Plant breeding is an extremely important route to genetic improvements that can increase yield and plant adaptability. Genetic improvement requires careful measurement of plant phenotypes or plant trait characteristics, but phenotype measurement is a tedious and error-prone task for humans to perform. High-throughput phenotyping aims to eliminate the problems of manual phenotype measurement. In this paper, we propose and demonstrate the efficacy of an automatic corn plant phenotyping system based on 3D holographic reconstruction. Point cloud image data were acquired from a time-of-flight 3D camera, which was integrated with a plant rotating table to form a screening station. Our method has five main steps: point cloud data filtering and merging, stem segmentation, leaf segmentation, phenotypic data extraction, and 3D holographic visualization. In an experimental study with five corn plants at their early growth stage (V3), we obtained promising results with accurate 3D holographic reconstruction. The average measurement error rate for stem major axis, stem minor axis, stem height, leaf area, leaf length and leaf angle were at 7.92%, 15.20%, 7.45%, 21.89%, 10.25% and 11.09%, respectively. The most challenging trait to measure was leaf area due to partial occlusions and rolling of some leaves. In future work, we plan to extend and evaluate the usability of the system in an industrial plant breeding setting.

1. Introduction

The growing world population and the lack of access to new arable land needed to maintain agricultural sustainability (Araus et al., 2008) is making plant breeding more important than ever before, as it can increase crop yield and plant adaptability. Genetic improvement in plant breeding focuses on exactly this problem, through selection for desired plant phenotypes during the plant breeding cycle (Poehlman and Sleper, 1995). Genetic improvement requires careful measurement of plant phenotypes, which is a tedious and error-prone task when done manually. High-throughput phenotyping is a new technique that returns a large quantity of data and addresses the problems of manual phenotyping, so it has recently received a great deal of attention for the plant trait discovery task (Cabrera-Bosquet et al., 2012; Furbank and Tester, 2011). High-throughput phenotyping uses various technologies, such as near-infrared spectroscopy spectral reflectance, photography, and sonar. For example, Khanna et al. (2011) used several spectral analyses to classify aquatic macrophytes species.

For many years, botanists have observed the structure of plants and proposed many models to describe plant parts. Some models describe overall structure, and some describe specific parts of plants. Furthermore, visualization of plant models has also been enhanced with computer graphics techniques. For example, Ijiri et al. (2005) developed 3D simulation of inflorescences, Ding et al. (2008) conducted 3D modeling of a plant structure, and Yao et al. (2010) proposed a flower blooming 3D model. However, this work has focused on general 3D models without exploiting the unique phenotypic characteristics of specific plants. Some groups of researchers produce 3D models of rice plant from images and barley plants from 3D sensors (Wernecke et al., 2007; Watanabe et al., 2005). Other researchers have developed methods for corn phenotype discovery and 3D visualization. Dornbusch et al. (2007) proposed a corn plant modeling procedure based on merging multiple 3D point cloud inputs and a mathematical model. Although they achieved excellent results, they did not perform automatic image capture and used only one single plant to demonstrate the use of the model. de Moraes Frasson and Krajewski

* Corresponding author at: Information Technology for Agriculture and Rural Development, Ubon Ratchathani University, Ubon Ratchathani 34190, Thailand. Tel.: +66 45 353500x2203, +66 84 6786750; fax: +66 45 288373.

E-mail addresses: supawadee.c@ubu.ac.th, supawadee.chaivivatrakul@ait.ac.th (S. Chaivivatrakul).

http://dx.doi.org/10.1016/j.compag.2014.09.005
0168-1699/

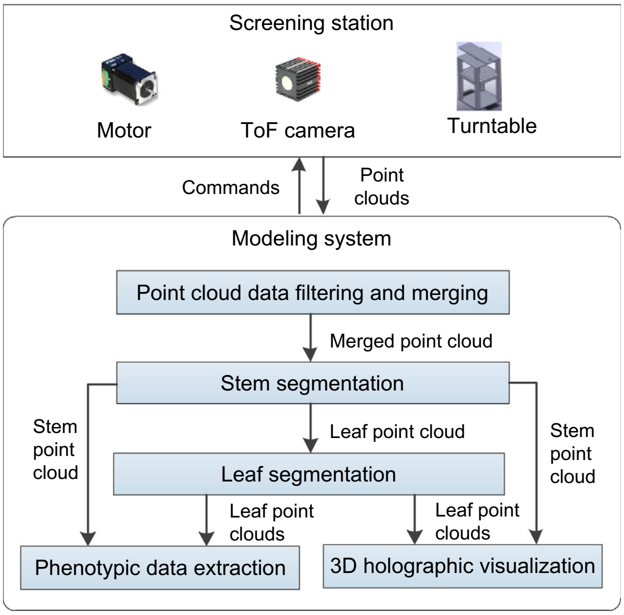

Fig. 1. Overview of the system, including screening system, modeling system, and main steps in modeling system.

(2010) also developed a 3D digital model of corn plants, but their method required attaching numerous markers to specific locations on a plant. None of the systems described in the literature are capable of fully automatic extraction of phenotypic data from their 3D models. The objective of the research reported upon in this paper was to develop a fully automatic system that is capable of characterizing corn plant morphological phenotypes in a controlled setting in a high-throughput fashion. These data include stem diameter, leaf length, leaf area, and leaf angle.

2. Materials and methods

An overview of our system is shown in Fig. 1. Our modeling system interacts with a plant screening station consisting of a time-of-flight (ToF) camera (SR-4000, MESA Imaging, Switzerland), a turntable, a stepper motor, and a computer station. The modeling system sends commands to the plant screening station, including commands to precisely rotate the turntable and to acquire a 3D point cloud at a specific viewing angle. After point cloud acquisition, we perform point cloud data filtering, merging, stem segmentation, leaf segmentation, phenotypic data extraction, and 3D holographic visualization. The output of each step is depicted in Fig. 2.

Fig. 3 shows the experimental screening station, with the SR-4000 camera facing the plant turntable. We performed an initial calibration to identify the point $\vec{p}_0$ (the center of the turntable's coordinate system at the top of the plant pot) in the camera coordinate system. The methods described in this report could be used with some modification for corn plants at other growth stages (up to V10, after which there will be tassels and fruits). For the purpose of algorithm validation, five corn plants at the representative V3 growth stage were used.

2.1. Point cloud data filtering and merging

The point cloud data filtering and merging step comprised five intermediate steps: acquiring input point clouds, filtering, rotation and transform, fine alignment using the iterative closest point (ICP) method, and filtering of the merged point cloud. The filtering, ICP, and merged point cloud filtering steps made use of the Point Cloud Library's (PCL) built-in functions (Rusu and Cousins, 2011). Fig. 5 shows sample results for each intermediate step of the process.

2.1.1. Acquiring input point clouds

For each predefined acquisition angle, we sent a command to rotate the turntable and then a command to acquire a 3D point cloud. To ensure that the plant would settle from vibrations before image acquisition, we inserted a one-minute interval between turntable rotation and point cloud acquisition. The data from the ToF camera were in an XYZ format according to the camera's Cartesian coordinate system, depicted in Fig. 4. The result of this step was a set of point clouds

$$P_{\theta_i,1} = \left\{\vec{p}^{\,j}_{\theta_i,1} = \left(x^j_{\theta_i,1}, y^j_{\theta_i,1}, z^j_{\theta_i,1}\right)\right\}_{1\leqslant j\leqslant N_{\theta_i}},$$

for various rotation angles $0 \leqslant \theta_i < 2\pi,\ 1 \leqslant i \leqslant N_{\theta_i}$. N_{θ_i} is the number of points in point cloud $P_{\theta_i,1}$, and N_θ is the total number of point clouds (acquisition angles).

2.1.2. Filtering

The point clouds generated by the ToF camera normally contained quite a few sparsely distributed outlier points. We used the statistical filtering algorithm of Rusu et al. (2008), which considers a point as either an inlier or an outlier based on the mean

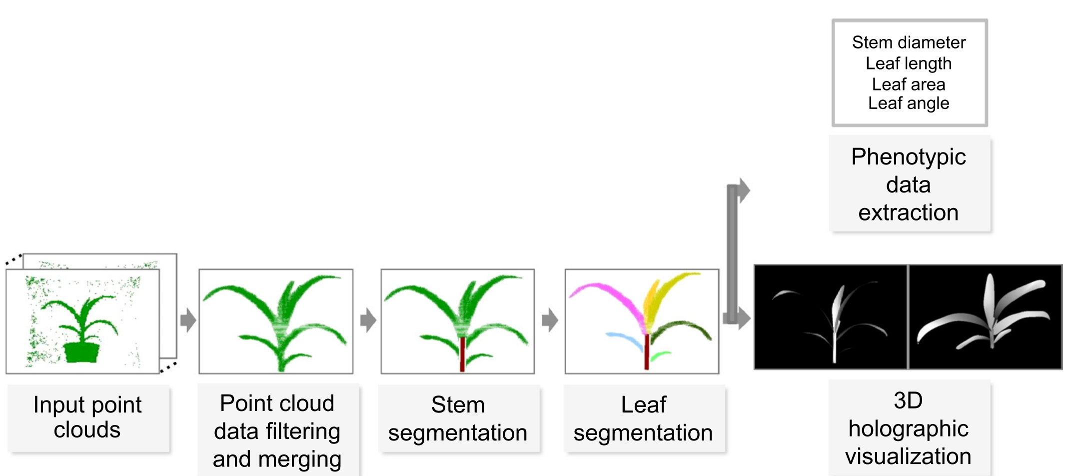

Fig. 2. Illustration of output of each main step in the modeling system.